AMERICAN SOCIETY FOR MICROBIOLOGY | Journal of Virology®

Studies on the Interaction of Tumor-Derived HD5 Alpha Defensins with Adenoviruses and Implications for Oncolytic Adenovirus Therapy

Charles Vragniau,[a,d] Jens-Martin Hübner,[a]* Peter Beidler,[a] Sucheol Gil,[a] Kamola Saydaminova,[a] Zhuo-Zhuang Lu,[a] Roma Yumul,[a] Hongjie Wang,[a] Maximilian Richter,[a] Pavel Sova,[a] Charles Drescher,[c] Pascal Fender,[d] André Lieber[a,b]

Division of Medical Genetics, University of Washington, Seattle, Washington, USA[a]; Department of Pathology, University of Washington, Seattle, Washington, USA[b]; Fred Hutchinson Cancer Research Center, Seattle, Washington, USA[c]; Institut de Biologie Structurale, CNRS/UGA/CEA, Grenoble, France[d]

ABSTRACT Defensins are small antimicrobial peptides capable of neutralizing human adenovirus (HAdV) *in vitro* by binding capsid proteins and blocking endosomal escape of virus. In humans, the alpha defensin HD5 is produced by specialized epithelial cells of the gastrointestinal and genito-urinary tracts. Here, we demonstrate, using patient biopsy specimens, that HD5 is also expressed as an active, secreted peptide by epithelial ovarian and lung cancer cells *in situ*. This finding prompted us to study the role of HD5 in infection and spread of replication-competent, oncolytic HAdV type 3 (HAdV3). HAdV3 produces large amounts of penton-dodecahedra (PtDd), virus-like particles, during replication. We have previously shown that PtDd are involved in opening epithelial junctions, thus facilitating lateral spread of *de novo*-produced virions. Here, we describe a second function of PtDd, namely, the blocking of HD5. A central tool to prove that viral PtDd neutralize HD5 and support spread of progeny virus was an HAdV3 mutant virus in which formation of PtDd was disabled (mut-Ad3GFP, where GFP is green fluorescent protein). We demonstrated that viral spread of mut-Ad3GFP was blocked by synthetic HD5 whereas that of the wild-type (wt) form (wt-Ad3GFP) was only minimally impacted. In human colon cancer Caco-2 cells, induction of cellular HD5 expression by fibroblast growth factor 9 (FGF9) significantly inhibited viral spread and progeny virus production of mut-Ad3GFP but not of wt-Ad3GFP. Finally, the ectopic expression of HD5 in tumor cells diminished the *in vivo* oncolytic activity of mut-Ad3GFP but not of wt-Ad3GFP. These data suggest a new mechanism of HAdV3 to overcome innate antiviral host responses. Our study has implications for oncolytic adenovirus therapy.

IMPORTANCE Previously, it has been reported that human defensin HD5 inactivates specific human adenoviruses by binding to capsid proteins and blocking endosomal escape of virus. The central new findings described in our manuscript are the following: (i) the discovery of a new mechanism used by human adenovirus serotype 3 to overcome innate antiviral host responses that is based on the capacity of HAdV3 to produce subviral penton-dodecahedral particles that act as decoys for HD5, thus preventing the inactivation of virus progeny produced upon replication; (ii) the demonstration that ectopic HD5 expression in cancer cells decreases the oncolytic efficacy of a serotype 5-based adenovirus vector; and (iii) the demonstration that epithelial ovarian and lung cancers express HD5. The study improves our understanding of how adenoviruses establish infection in epithelial tissues and has implications for cancer therapy with oncolytic adenoviruses.

KEYWORDS adenovirus, cancer, defensins, innate immunity

Received 13 October 2016 **Accepted** 20 December 2016

Accepted manuscript posted online 11 January 2017

Citation Vragniau C, Hübner J-M, Beidler P, Gil S, Saydaminova K, Lu Z-Z, Yumul R, Wang H, Richter M, Sova P, Drescher C, Fender P, Lieber A. 2017. Studies on the interaction of tumor-derived HD5 alpha defensins with adenoviruses and implications for oncolytic adenovirus therapy. J Virol 91:e02030-16. https://doi.org/10.1128/JVI.02030-16.

Editor Lawrence Banks, International Centre for Genetic Engineering and Biotechnology

Address correspondence to André Lieber, lieber00@uw.edu.

* Present address: Jens-Martin Hübner, Division of Pediatric Neuro-oncology, German Cancer Research Center, Heidelberg, Germany.

C.V. and J.-M.H. contributed equally to this article.

Defensins are small, cationic antimicrobial peptides that are characterized by several disulfide bonds and can, depending on the spatial distribution of the cysteine residues and connectivity of disulfide bonds, be divided into the subfamilies of alpha, beta, and theta defensins. So far, six alpha defensins that can be further distinguished as being of myeloid (human neutrophil peptide 1 [HNP-1], HNP-2, HNP-3, and HNP-4) or epithelial (human defensin 5 [HD-5] and HD-6) origin and 31 beta defensins have been found in humans (1).

Defensins show broad antiviral activity against both enveloped and nonenveloped viruses (2). For example, defensins can inhibit infection by cytomegalovirus (CMV), human immunodeficiency virus (HIV), human parainfluenza virus (HPIV), herpes simplex virus (HSV), influenza A virus (IAV), respiratory syncytial virus (RSV), vesicular stomatitis virus (VSV), vaccinia virus (VV), adeno-associated virus (AAV), human papillomavirus (HPV), and human adenovirus (HAdV) species A, B, C, and E (but not infection by species D and F) (3). HD5 binds to the capsids of sensitive HAdV serotypes and forms a bridge between extruding penton base loops and regions in the fiber, thus cementing the fiber into the capsid (3, 4). This capsid stabilization prevents the release of the endosomolytic protein VI and exposure of the internal core viral DNA, subsequently blocking endosome escape, nuclear localization, and ultimately replication of adenovirus (Ad) in infected cells.

HNP-1, -2, -3, and -4 are produced in neutrophils, granulocytes, and specific lymphocyte and monocyte subpopulations. Peptides HNP-1 to HNP-4 were found in lung cancer, oral squamous carcinoma, bladder cancer, renal cell carcinoma, colorectal cancer, breast cancer, cutaneous T-cell lymphoma, basal cell carcinoma, and invasive as well as head and neck cancer (for a review, see reference 5). It is thought that signals of HNP-1 to HNP-4 originate from tumor-infiltrating leukocytes. It was reported that HNP-1 to HNP-4 can support tumor growth through induction of the epithelial-to-mesenchymal transition, thus increasing tumor invasiveness (6, 7), as well as through attraction of tumor-associated macrophages that support tumor growth (8).

The association of the alpha defensin HD5 with cancer is less studied. HD5 is predominantly produced by and secreted from Paneth cells, specialized epithelial cells in the gastrointestinal (GI) tract (5). In Paneth cells, HD5 is primarily secreted as a precursor molecule and then undergoes proteolytic processing by Paneth cell-derived trypsin to generate mature forms with antimicrobial activity (9). The molecular masses for pro-HD5 forms are 8.1, 7.7, and 7.0 kDa (9). The molecular masses for mature HD5 forms are 4.3 and 3.6 kDa. HD5 expression has also been detected in epithelial cells of the urinary (10) and reproductive (11) tracts where HD5 is thought to contribute to the innate immune protection from pathogens. For HD5 produced in the genito-urinary tract, the key processing and activating enzymes are neutrophil-derived proteases (12). Although there are no reports of airway epithelial cells expressing HD5, the epithelial lining fluid of the lung contains 0.3 μM HD5, suggesting a potential function in blocking microbes in the airway tract (13). Two studies report that HD5 peptide is present in colon cancer and most likely produced by malignant Paneth cells (14, 15). HD5 expression was also documented in the colon cancer cell line Caco-2 where HD5 gene expression can be increased by recombinant fibroblast growth factor 9 (FGF9) (16). Because HD5 is found in other epithelial tissues, it is thought that it is produced by epithelial cancers other than colon cancer (5). We have corroborated this by our studies with human ovary, endometrium, and lung cancer samples. HD5 expression in tumors prompted our study on the effect of HD5 on oncolytic adenovirus therapy.

Oncolytic virotherapy focuses on engineering viruses in a way that they infect cancer cells and replicate and spread their progeny to neighboring tumors cells, eventually eliminating the tumor (17). Most clinically used oncolytic adenoviruses were based on species C serotype 5 (HAdV5). HAdV5 uses the coxsackie adenovirus receptor (CAR) as a primary attachment receptor. Because CAR expression on cancer cells is variable, HAdV serotypes with tropism other than CAR are being explored for oncolytic virus therapy. Among them are vectors derived from species B serotypes HAdV3 and -11 (18, 19). These serotypes use desmoglein 2 (DSG2) as a receptor.

During HAdV infection, the penton base and fiber proteins are produced in excess and assembled in the cytosol to form fiber-penton base hetero-oligomers called pentons (20, 21). In the cases of HAdV3, -11, and -14, 12 pentons self-assemble into dodecamers (penton-dodecahedra [PtDd]) with a diameter of ~30 nm (22). During HAdV3 replication, PtDd are formed at an excess of 5.5×10^6 PtDd per infectious virus (22). Dodecamerization of pentons is required for high-affinity binding to DSG2. PtDd are released from Ad-infected cells before virus-triggered cytolysis and can be found in the paracellular space in epithelial cell cultures. We have recently shown that PtDd produced early during viral infection transiently open intercellular junctions between epithelial cells and thus facilitate the lateral spread of *de novo*-produced virions (23, 24). PtDd binding to DSG2 causes clustering of several DSG2 molecules, which in turn triggers intracellular signaling that culminates in junction opening. This mechanism involves the phosphorylation of mitogen-activated protein (MAP) kinases, triggering the activation of the matrix metalloproteinase ADAM17. ADAM17 in turn cleaves the extracellular domain of DSG2 that links epithelial cells together (25).

The central goal of this study was to demonstrate that PtDd are also capable of neutralizing defensin HD5, which represents a barrier to HAdV3 infection and dissemination. As a tool, we used a previously generated HAdV3 mutant (23). Based on the three-dimensional (3D) structure of Ad3 PtDd, we introduced a double mutation (D100R and R425E) into the penton base sequence of Ad3 that would break up the salt bridge between two neighboring pentons and prevent the assembly of PtDd. The penton base mutant (mut-Ad3GFP) is identical to its wild-type counterpart (wt-Ad3GFP) in the efficiency of progeny virus production; however, it is disabled in the production of PtDd.

RESULTS

HD5 is expressed in epithelial ovarian cancer. To provide therapeutic relevance for our studies on the interaction between HAdV and HD5, we investigated HD5 expression in normal and malignant ovarian tissues. Compared to normal tissue, HD5 mRNA expression was upregulated in endometrioid and serous ovarian cancer biopsy specimens (Fig. 1A). To exert its antiviral activity, HD5 has to be produced as an active protein. We used Western blot and immunohistochemistry (IHC) analyses to demonstrate this.

In our Western blot studies, recombinant mature HD5 ran at a molecular mass of ~4 kDa. In the same range, we detected signals in three out of nine endometrioid cancer biopsy specimens and one out of seven serous ovarian cancer biopsy specimens (Fig. 1B, lanes 4, 5, 8, and 16). In the same samples, signals in the range of 6.6 to 8 kDa, which could represent pre-HD5 forms (9), were visible. In some biopsy specimens, processed forms with different molecular masses were detected (Fig. 1B, lanes 3, 6, and 8), while in other biopsy specimens only the ~8-kDa pro-HD5 form was observed (Fig. 1B, lanes 9, 12, and 14). There was also immunoreactivity with proteins larger than 14 kDa, which, at this point, cannot be explained. Only one out of nine biopsy specimens of healthy ovarian tissue displayed signals that resembled HD5. In summary, the Western blot studies indicated that in ovarian cancer HD5 protein is expressed as its precursor form. In most endometrioid cancer biopsy specimens, HD5 is processed to mature peptides. Processing products can differ in individual tumors.

Furthermore, we performed IHC for HD5 on formalin-fixed paraffin and frozen tissue sections. The HD5 specificity of the monoclonal anti-HD5 antibody used was confirmed on sections of healthy colon, where signals were localized to Paneth cells (Fig. 2A). HD5 staining was found in sparse epithelial cells on sections of healthy or premalignant endometrial tissues (Fig. 2B and C, respectively). In contrast, sections of malignant endometrioid ovarian cancer tissue showed strong HD5 immunoreactivity (Fig. 2D to I). HD5 staining was found inside malignant cells (Fig. 2E, G, and I) and in the tumor stroma (Fig. 2F and H), which could represent secreted HD5. The intensity of HD5 reactivity varied between patients (Fig. 2D to F for patient 1, G for patient 2, and H and I for patient 3). To demonstrate that HD5 is produced by epithelial cancer cells, we

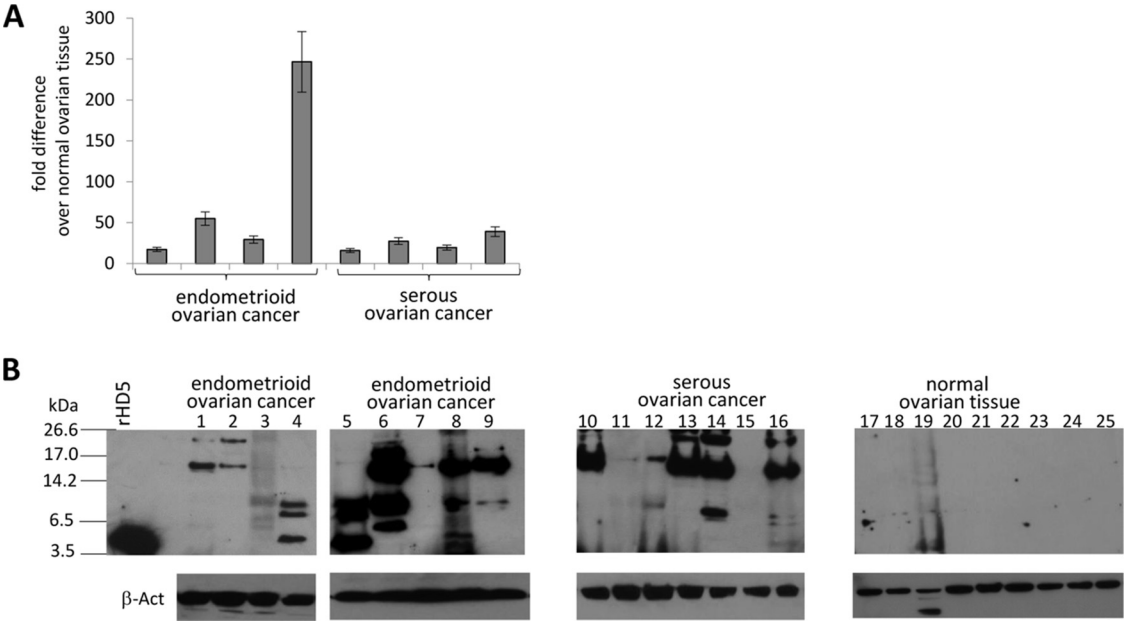

FIG 1 HD5 expression in ovarian cancer biopsy specimens from patients. (A) Fold increase of HD5 mRNA levels in endometrioid and serous ovarian cancer biopsy specimens compared to levels in healthy ovarian tissue pooled from five patients. HD5 mRNA levels were measured by qRT-PCR and normalized to the level of β-actin mRNA. Each column represents a biopsy specimen from an individual patient. The standard deviation is derived from technical repeats ($n = 3$). (B) Western blot analysis for HD5 in tissue samples. Each lane represents an individual biopsy specimen. rHD5, 100 ng of recombinant HD5. After HD5 Western blotting, filters were stripped and incubated with antibodies against β-actin as a loading control.

costained frozen sections with antibodies against HD5 and DSG2, an epithelial junction protein (Fig. 3A). These results were confirmed by staining of consecutive paraffin sections with antibodies against HD5 and DSG2, respectively (Fig. 3B).

HD5 is expressed in small-cell lung cancer. Furthermore, we performed IHC for HD5 on paraffin sections from small-cell lung cancer tissues. In all three patients, we found strong HD5 signals (Fig. 4). HD5 appeared to be produced by malignant cells, and the secreted form accumulated in tumor stroma and necrotic areas.

Our findings that secreted HD5 is produced by ovary, endometrium, and lung cancers creates a basis to further study the implication of cancer-derived HD5 for oncolytic adenovirus therapy.

Effect of synthetic defensins on adenovirus infection and spread. In agreement with studies by Smith et al. (3), we demonstrated that synthetic HD5 defensin inhibited the transduction of a cancer cell line by HAdV5 and HAdV3 vectors (Fig. 5A). We used replication-competent vectors expressing green fluorescent protein (GFP) (wt-Ad5GFP and wt-Ad3GFP, respectively, where wt is wild type, and preincubated them with a synthetic HD5 peptide. The mixture was then added to lung cancer A549 cells, and GFP fluorescence was analyzed 48 h later. While transduction with wt-Ad5GFP was completely blocked by HD5, this effect was less pronounced for wt-Ad3GFP. We then compared viral spread of wt-Ad3GFP and the penton base mutant mut-Ad3GFP. The two viruses contain identical GFP expression cassettes to follow transduced cells (Fig. 5B). Infection of cells, viral replication, and production of penton base were comparable for both viruses (23). wt-Ad3GFP and mut-Ad3GFP viruses were used to infect confluent A549 cells at a multiplicity of infection (MOI) of 0.5 PFU/cell. Culture medium was changed every day either without or with 15 μM HD5. Cell viability was assessed either by crystal violet staining (Fig. 5C) or MTT (3-[4,5-dimethyl-2-thiazolyl]-2,5-diphenyl-2H-tetrazolium bromide) assay (Fig. 5D) at day 5 after infection. In the absence of HD5, both viruses efficiently killed the monolayer of A549 cells as a result of viral spread, whereby mut-Ad3GFP was slightly less potent (3% remaining viable cells for wt-Ad3GFP versus 9% viable cells for mut-Ad3GFP; $P < 0.05$), most likely as a result of its reduced

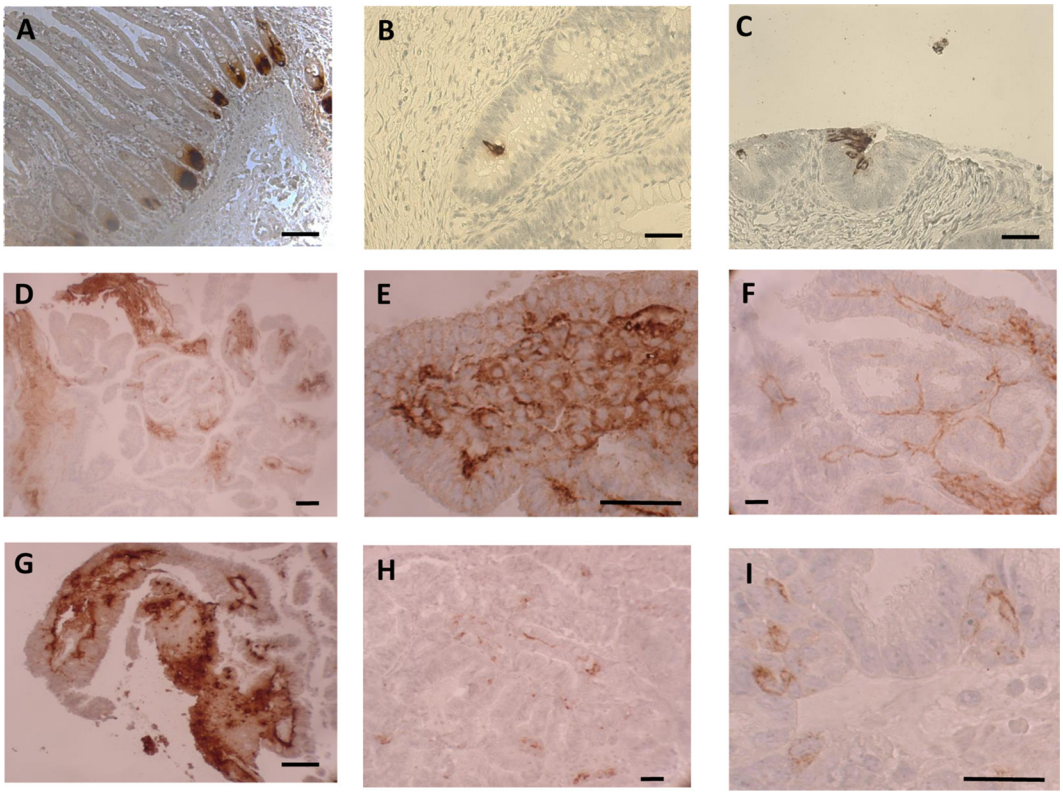

FIG 2 Immunohistochemistry for HD5 on formalin-fixed paraffin sections. HD5 staining appears in brown. (A) Normal colon tissue. (B) Healthy endometrial tissue. (C) Tissue showing complex atypical hyperplasia, which is a premalignant lesion of endometrial origin. (D to I) Tissues from patients with endometrioid ovarian cancer, as follows: patient 1, panels D to F; patient 2, panel G; patient 3, panels H and I. Scale bar, 50 μm.

ability to open epithelial junctions that formed between A549 cells. Addition of HD5 slightly diminished the potency of wt-Ad3GFP (22% remaining viable cells), indicating that PtDd cannot completely inactivate HD5 at the concentration used. Importantly, the cytolytic activity of mut-Ad3GFP was nearly completely blocked in the presence of HD5 ($P < 0.001$ for the difference between results for wt-Ad3GFP with HD5 and mut-Ad3GFP with HD5). The data support our hypothesis that PtDd released from primary infected cells act as a decoy for HD5 present in paracellular spaces and thus facilitate secondary infection and spread of *de novo*-produced wt-Ad3GFP.

Binding of HD5 to PtDd. The above hypothesis suggests that PtDd binds to HD5. In an attempt to demonstrate this, we first used a surface plasmon resonance (SPR) assay (Fig. 6A). HD5 was immobilized on sensor chips, and different concentrations of recombinant PtDd were injected. A dose-response effect was clearly observed, confirming PtDd interaction with immobilized HD5. However, affinity assessment was not possible, and nonphysiological avidity might be partly responsible for the slow dissociation phase. As a second method, we used a Western blot assay where we separated PtDd, HAdV3 fiber knob, and wt-Ad3GFP virus on an SDS-polyacrylamide gel, blotted the proteins, and incubated the filters with synthetic HD5 peptides as a probe (Fig. 6B). HD5 binding was detected using a rat polyclonal anti-HD5 antibody followed by an anti-rat IgG-horseradish peroxidase (HRP) conjugate (Fig. 6B, Western panels). Before being loaded on the gel, samples were either boiled for 5 min in the presence of β-mercaptoethanol or left unboiled (Fig. 6B, B or UB, respectively). In the lanes representing boiled PtDd, the 62-kDa penton base monomer and the 27-kDa fiber monomer are visible. HD5 binds to both proteins, as well as a smaller (~58-kDa) protein which is most likely a penton base derivative. HD5 binding to the penton base proteins is also detected in lanes in which complete wt-Ad3GFP virions were loaded. Here, binding to the fiber might be below the detection limit of the assay in the unboiled

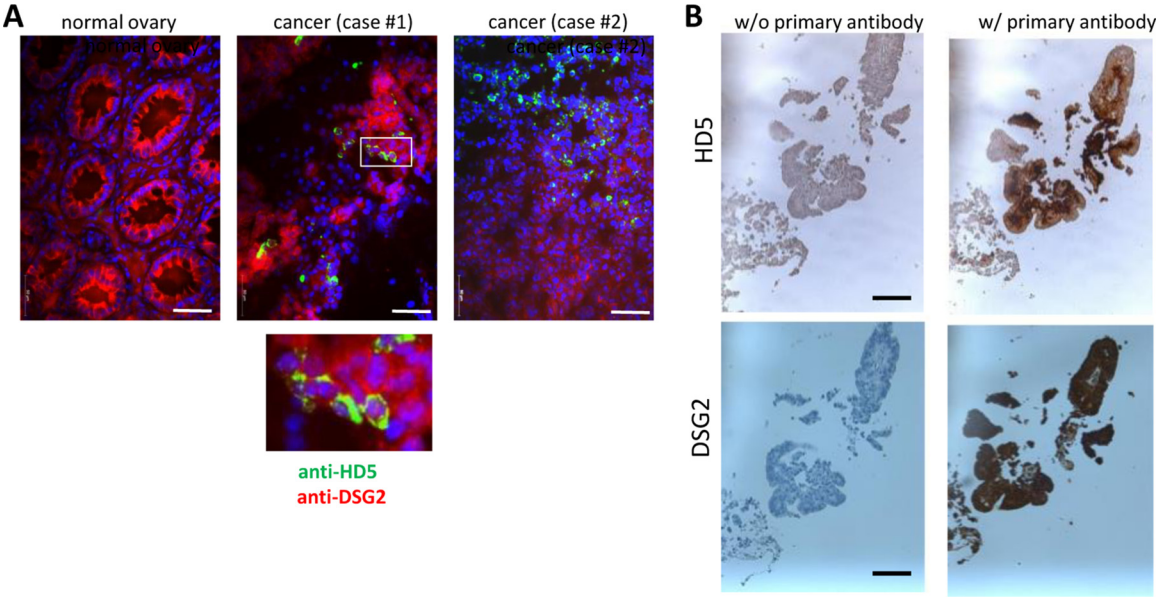

FIG 3 Colocalization of HD5 and DSG2 in ovarian cancer sections. (A) Immunofluorescence analysis for HD5 (green) and desmoglein 2 (DSG2) (red) on sections from biopsy specimens of normal ovarian tissues and two cases of endometrioid ovarian cancer. The small panel is a 5-fold-magnified image of the area boxed in white and shows that HD5 signals are present in DSG2-positive cancer cells. (B) Staining of consecutive paraffin sections with HD5- and DSG2-specific antibodies. (Left panels) As controls, sections were incubated without (w/o) the primary anti-HD5 or anti-DSG2 antibody and with the corresponding HRP-conjugated secondary antibody only. (Right panels) Sections were stained with primary and secondary antibodies. Scale bar, 50 μm.

sample (Fig. 6B, UB lane of Ad3 virus). No other virus capsid protein appeared to interact with HD5, including the most abundant capsid protein hexon (~97 kDa). For both PtDd and wt-Ad3GFP virions, signals at ~90 kDa or ~150 kDa were visible in the lanes representing unboiled samples. These signals could represent multimeric penton base protein forms that were not completely dissociated into monomers. Smith et al. reported that HD5 binding involves the fiber shaft and the penton base (26). In our study, we found strong HD5 binding signals to a recombinant protein consisting of one Ad3 shaft motif and the Ad3 fiber knob (Fig. 6B, Ad3 knob).

Effect of endogenously induced HD5 gene expression on viral spread and the role of PtDd. So far, our studies involved synthetic HD5 peptide added to virus or cells. Next, we attempted to show that PtDd can neutralize endogenously expressed HD5 and thus increase viral spread. To do this, we capitalized on a report that recombinant FGF9 induced HD5 mRNA and protein expression in human colon cancer Caco-2 cells (16). FGF9 triggers signaling through FGF receptor 3 (FGFR-3), and the HD5 gene is a downstream target of FGFR-3. We measured HD5 mRNA levels by quantitative reverse transcription-PCR (qRT-PCR) in three human cancer cell lines incubated with or without FGF9 for 4 days (Fig. 7A). In Caco-2 cells we found an ~150-fold increase in HD5 mRNA levels upon FGF9 incubation. In another human colon cancer cell line, T84, FGF9 increased HD5 mRNA levels ~9-fold. HD5 mRNA was not detectable in cervical carcinoma HeLa cells with or without FGF9 incubation. The levels of secreted HD5 protein in tissue culture supernatants of Caco-2 and T84 cells were induced 22-fold and 2.4-fold, respectively, by FGF9, as measured by enzyme-linked immunosorbent assay (ELISA) (Fig. 7B). We then infected FGF9-treated and -untreated Caco-2, T84, and HeLa cells with wt-Ad3GFP or mut-Ad3GFP and measured the titers of *de novo*-produced virus in two assays. The first assay measured GFP-expressing units (infectious units [IU]) in culture supernatants after infection of 293 cells with 1:100 dilutions of cell supernatants (Fig. 7C). While the titers of *de novo*-produced Ads were comparable in cells without FGF9, they were significantly lower for mut-Ad3GFP generated in FGF9-treated Caco-2 and T84 cells ($P < 0.001$). The PtDd-producing wt-Ad3GFP, however, was not affected by FGF9-mediated HD5 expression. There was no effect of FGF9 on the titers

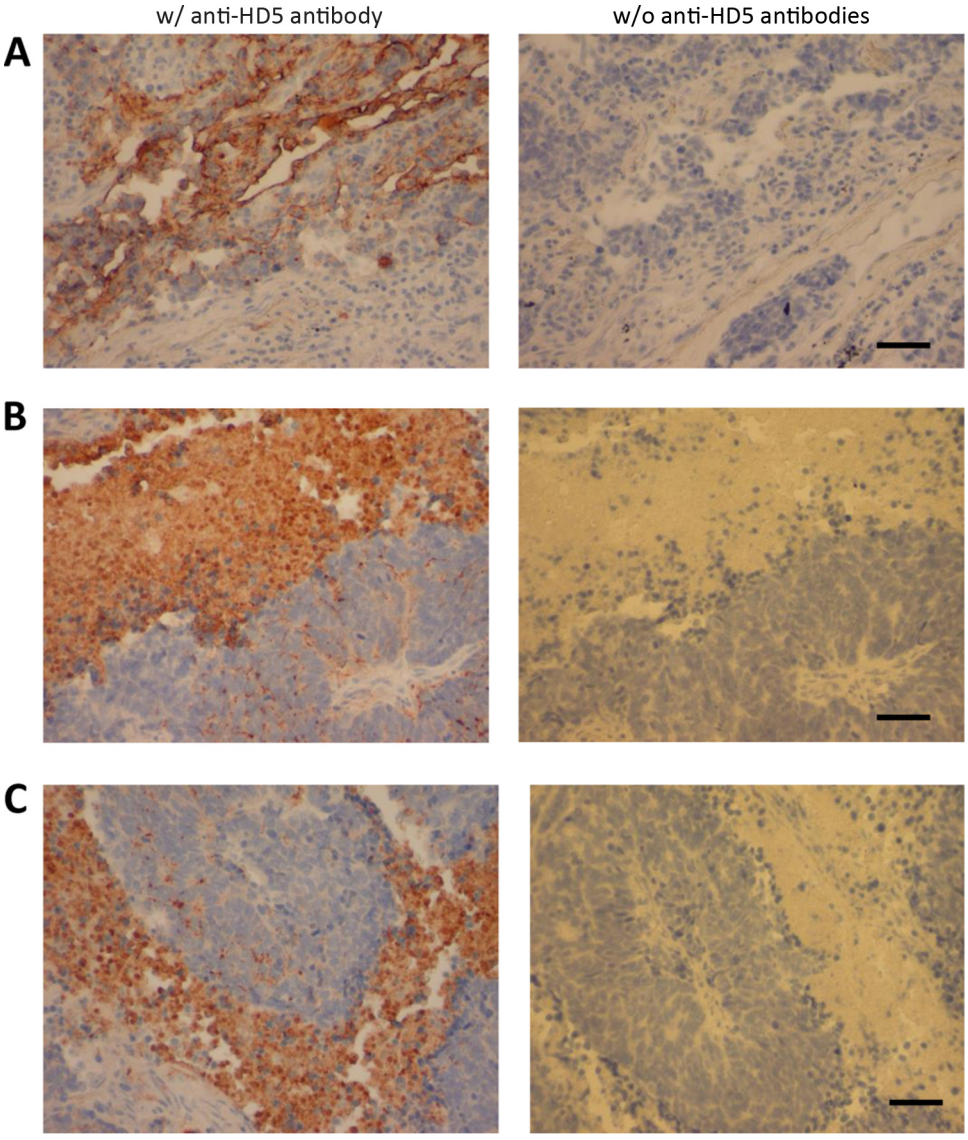

FIG 4 Immunohistochemistry for HD5 on formalin-fixed paraffin sections of small-cell lung cancer tissue. HD5 staining appears in brown. Images in panels A to C are from three different biopsy specimens/patients. In panels B and C accumulation of HD5 in tumor stroma can be seen. Scale bar, 50 μm.

of either virus in HeLa cells, which do not produce HD5. To consolidate these data, viral genome titers were measured in Caco-2 cell lysates by quantitative PCR (qPCR) (Fig. 7D). As seen in the infectious-unit assay, titers of mut-Ad3GFP produced in FGF9-treated Caco-2 cells were significantly lower ($P < 0.05$) although the differences in the cell lysates were not as substantial as seen in the infectious-unit assay of the supernatants. The outcome of these studies is summarized in Fig. 7E. wt-Ad3GFP produces PtDd, which block FGF9-induced HD5. For wt-Ad3GFP, there was no difference in transduction and spread in the presence or absence of FGF9. mut-Ad3GFP does not produce PtDd and is therefore not capable of blocking FGF9-induced defensins. Viral spread and progeny virus production were blocked for mut-Ad3GFP. Our data also suggest that Caco-2 cells can cleave pro-HD5 into active forms. This is in line with previous reports that colon cancers express proteases capable of cleaving HD5 (14, 15).

Effect of ectopically expressed HD5 on *in vivo* oncolytic efficacy of wt-Ad5GFP, wt-Ad3GFP, and mut-Ad3GFP. To further test our hypothesis and assess whether our findings are relevant for cancer therapy with oncolytic adenoviruses, we generated isogenic tumor cell lines with expression of an ectopic HD5 gene. We first screened

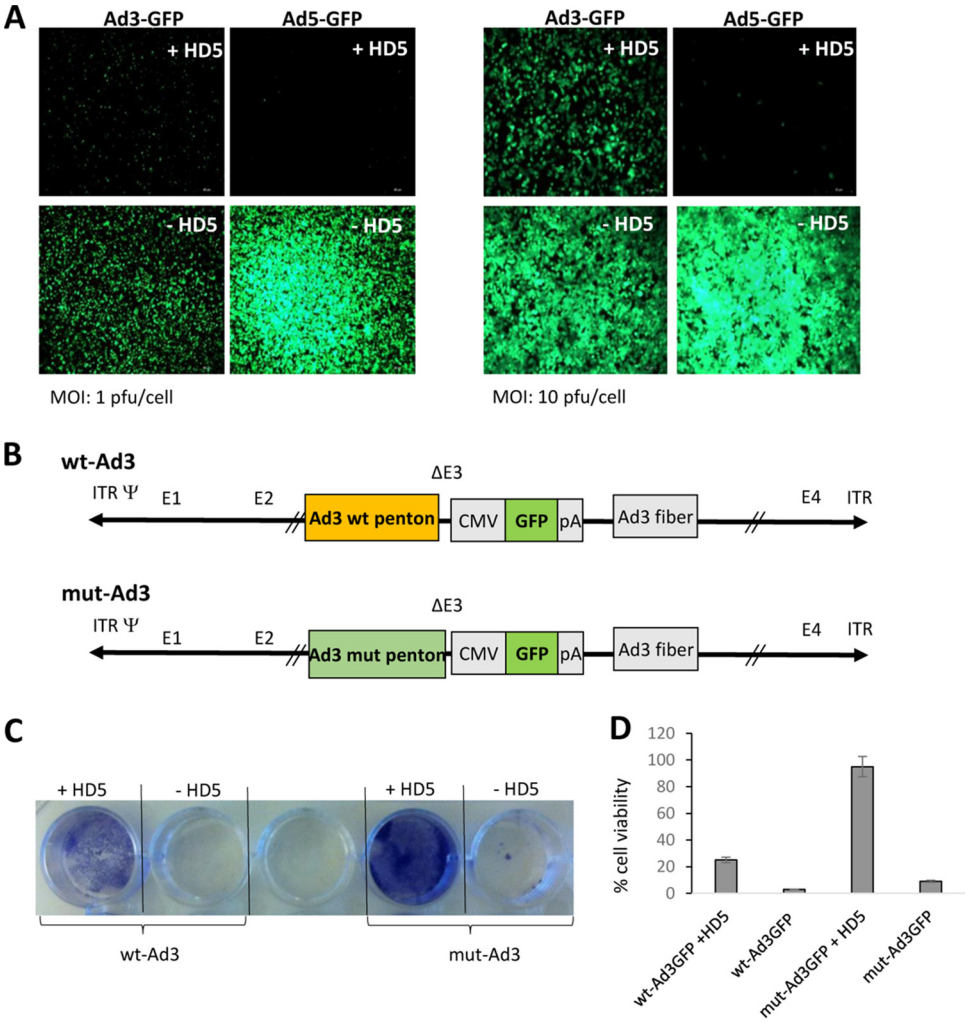

FIG 5 Inhibition of adenoviral infection and spread by synthetic HD5. (A) Inhibition of transduction. Replication-competent wt-Ad3GFP and wt-Ad5GFP were preincubated with 15 μM synthetic HD5 peptide or scrambled control peptide for 1 h at 4°C. The mixture was then added to A549 cells at an MOI of 1 or 10 PFU/cell in serum-free medium for 2 h at 37°C. Cells were washed, and fresh medium was added to cells. After 48 h, transduction was analyzed based on GFP fluorescence. Representative images are shown. Scale bar, 50 μm. (B) mut-Ad3GFP is identical to wt-Ad3GFP except for the two D100R and R425E amino acid substitutions in the penton base that disable the assembly of penton base and fiber into PtDd. This mutation does not decrease the level of penton base production or virus titers. ITR, inverted terminal repeat; pA, polyadenylation sequence. (C) Inhibition of mut-Ad3GFP spread. Confluent A549 cells in DMEM and 1% FBS were infected at an MOI of 0.5 PFU/cell for 2 days with wt-Ad3GFP or mut-Ad3GFP. At day 2, 15 μM synthetic HD5 peptide or scrambled control peptide was added daily for 5 days after medium change. Viable cells were stained with crystal violet at day 5. Representative images are shown. (D) Inhibition of mut-Ad3GFP spread. A549 cells were treated as described for panel C, and cell viability was measured 5 days after addition of HD5 by MTT assay. Cell viability of uninfected/untreated cells was taken as 100% ($n = 3$).

human cancer cell lines for endogenous HD5 mRNA expression. These included the lung cancer cell line A549, the breast cancer cell line BT474, HEK 293 cells, the erythroleukemia cell line K562, and the lymphoma cells lines Raji and Farage. For comparison, we also included human peripheral blood mononuclear cells (PBMCs) (Fig. 8A). Overall, HD5 mRNA levels were relatively low, i.e., 0.01 to 0.3% of β-actin mRNA levels. Interestingly, HD5 mRNA levels were relatively high in both lymphoma cell lines. The lowest HD5 mRNA levels were found in BT474 and K562 cells. We therefore focused on these cell lines. The HD5 gene under the control of the strong ubiquitously active elongation factor alpha (EF1α) promoter was transferred into cells by a VSV-G-pseudotyped lentivirus vector (Fig. 8B, upper panel). Transduced cells were selected with G418 for 4 weeks. HD5 mRNA levels, measured by qRT-PCR,

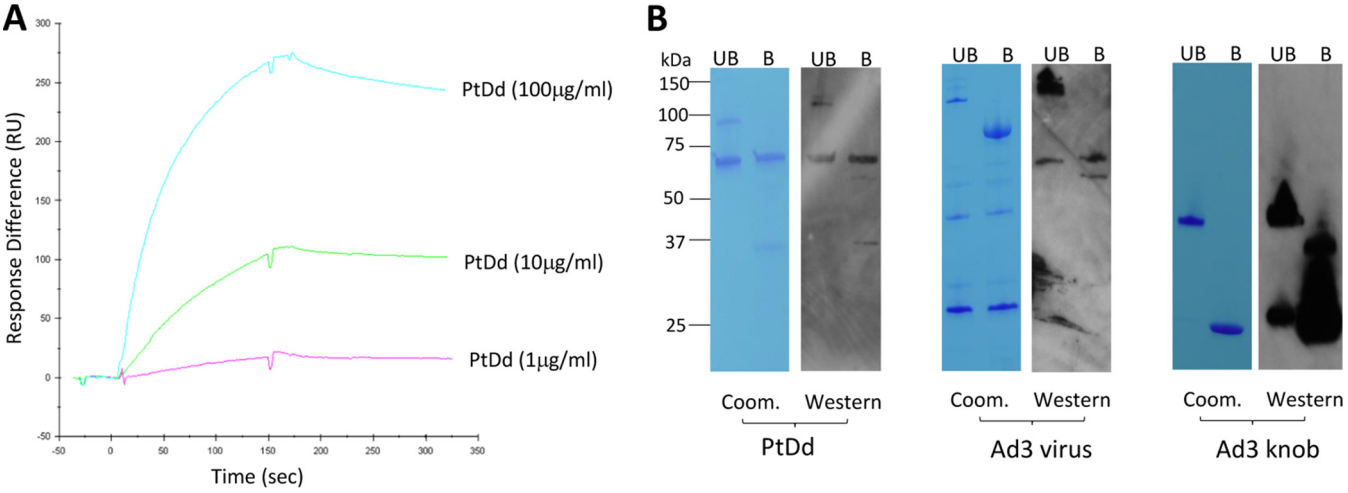

FIG 6 Binding of HD5 to PtDd. (A) Surface plasmon resonance analysis. HD5 was immobilized on sensor chips, different concentrations of recombinant PtDd (1, 10, and 100 μg/ml) were injected, and the response curves were recorded. (B) Binding of HD5 in Western blot assays. One microgram of recombinant PtDd, 1 μg of Ad3 fiber knob, or 10^9 PFU of wt-Ad3GFP virus in Laemmli buffer was either directly loaded or boiled for 5 min in the presence of 2-mercaptoethanol before being loaded on an SDS-polyacrylamide gel. After electrophoresis, proteins were either stained with Coomassie blue (left panels) or blotted to a PVDF membrane which was then incubated with 0.1 μM synthetic HD5 peptide. HD5 binding was detected by a polyclonal anti-HD5 antibody (right panels). The theoretical molecular masses of Ad3 hexon, penton base, and fiber monomers are 97, 61.8, and 34.8 kDa, respectively. The molecular mass of the monomeric recombinant Ad3 fiber knob is 23 kDa. The fiber knob forms relatively stable trimers.

were ~5- and 4-fold higher, respectively, in K562 and BT474 cells transduced with the HD5 lentivirus vector than in the parental cell line (Fig. 8B, lower panels). Growth of BT474 cells expressing HD5 slowed down greatly, which made it difficult to obtain the cell numbers required for *in vivo* studies. We therefore focused on the erythroleukemia cell lines K562 and K562 cells expressing HD5 (K562-HD5). The use of a nonepithelial cell line would also allow a focus on the HD5-neutralizing function of PtDd without interference by the junction-opening function of PtDd. Production of secreted HD5 protein in K562-HD5 cells was confirmed by ELISA (Fig. 8C). While immunoreactive HD5 was secreted from K562-HD5 cells into the supernatant, it was not processed into active forms, and spread of mut-Ad3GFP was not decreased by HD5 in confluent K562-HD5 cultures (data not shown).

To establish tumors, 2 million K562 or K562-HD5 cells in Matrigel were injected subcutaneously into immunodeficient mice. Immunohistochemistry of tumors showed infiltration of mouse leukocytes (Fig. 9A). When tumors reached a volume of 200 mm^3, wt-Ad3GFP or mut-Ad3GFP was injected intratumorally, and tumor volumes were measured (Fig. 9B). Expression of HD5 in K562 cells had no effect on tumor growth. wt-Ad3GFP delayed the growth of K562 and K562-HD5 tumors to similar degrees. A comparable antitumor effect was observed for mut-Ad3GFP injected into K562 tumors. Notably, the erythroleukemia cell line K562 does not form epithelial junctions, and PtDd is therefore not necessarily required to overcome this barrier to viral spread. However, the expression of HD5 in K562-HD5 tumors significantly inhibited the oncolytic activity of mut-Ad3GFP ($P < 0.01$ at day 19). The inhibitory effect of HD5 expression on mut-Ad3GFP was abolished by intratumoral injection of recombinant PtDd (Fig. 9C). The study showed similar levels of antitumor efficacy between the K562-HD5 cells injected with mut-Ad3GFP and treated with PtDd and the K562 cells injected with mut-Ad3GFP. This indicates that HD5 expression negatively affects the oncolytic activity of Ads that do not produce PtDd. To further support this, we performed a study with the replication-competent wt-Ad5GFP vector as a prototype for an HAdV5-based oncolytic virus (Fig. 9D). wt-Ad5GFP was injected into K562 and K562-HD5 tumors as described for the Ad3 study, and tumor volumes were measured at day 19 after tumor cell implantation. Our data show that wt-Ad5GFP-injected K562 tumors were significantly smaller than wt-Ad5GFP-injected K562-HD5 tumors, suggesting that HD5 blocks the oncolytic activity of wt-Ad5GFP.

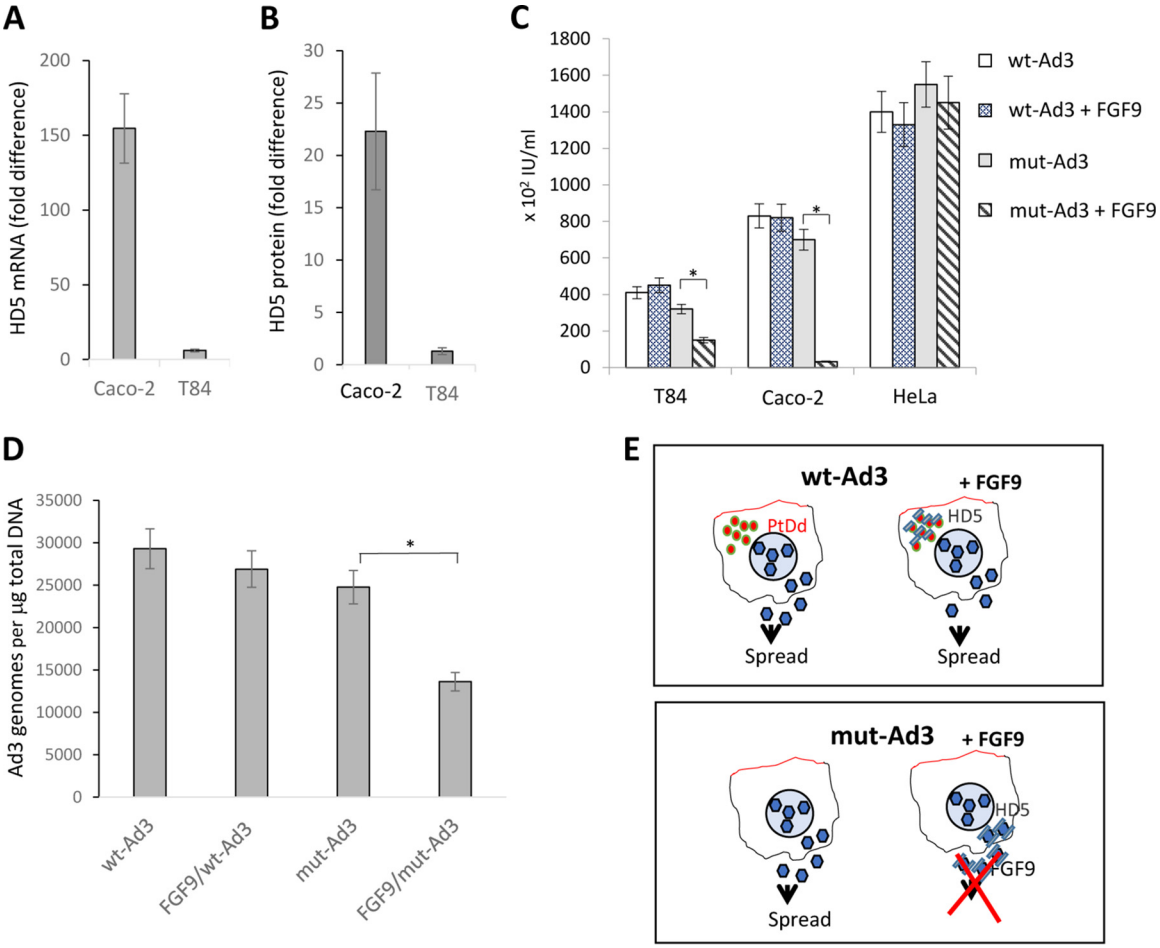

FIG 7 Role of PtDd in blocking HD5-mediated virus inactivation. (A) Induction of HD5 mRNA expression by FGF9. Colon cancer Caco-2 and T84 cells were incubated with FGF9 (50 ng/ml) for 3 days. Then, total RNA was purified, and HD5 mRNA was measured by qRT-PCR. Shown is the fold change in levels of HD5 mRNA compared to the level in untreated cells. HD5 mRNA levels in FGF9-treated and -untreated cells were normalized to β-actin mRNA levels ($n = 3$). (B) HD5 protein levels in culture supernatant after FGF9 induction measured by ELISA. Shown is the fold change of HD5 concentrations relative to those in untreated cells ($n = 3$). (C) Titration of progeny virus in cells in which HD5 expression was induced by FGF9. Confluent T84, Caco-2, or HeLa cells were used for these studies. One set of wells was treated daily (after medium change) with FGF9 (50 ng/ml). After 4 days of FGF9 treatment, wt-Ad3GFP and mut-Ad3GFP were added at an MOI of 0.5 PFU/cell for 2 h, followed by a medium change. Medium (with and without FGF9) was changed daily. Medium aliquots were collected at day 4 after infection and filtered to remove detached cells, and titers (infectious units [IU]) were determined on GFP-expressing 293 cells. Only differences between results for the wt-Ad3GFP FGF9-treated and -untreated groups were significant (*, $P < 0.001$; $n = 3$). (D) Quantification of viral genomic DNA in Caco-2 cell lysates. Cells were collected after 4 days of FGF9 treatment as described for panel C. Genomic DNA was isolated, and Ad3 genomes were measured by qPCR using hexon primers. Only differences between results for the mut-Ad3GFP FGF9-treated and -untreated groups were significant ($n = 3$; *, $P < 0.05$). (E) Diagram explaining the decreased spread of mut-Ad3GFP in FGF9-induced cells. wt-Ad3GFP produces PtDd which neutralize FGF9-induced HD5. Therefore, there was no significant difference in wt-Ad3GFP spread and progeny production in the presence or absence of FGF9. mut-Ad3GFP does not form PtDd and is therefore incapable of inactivating HD5 and protecting progeny virus. mut-Ad3GFP progeny virus production is therefore inhibited in FGF9-treated cells.

DISCUSSION

The expression of HD5 mRNA and protein in colon cancer has been reported previously (14, 15). In our study, we demonstrate the presence of processed HD5 peptides in epithelial ovarian cancer, predominantly in cases of endometrioid cancer. We speculate that HD5 processing is mediated by proteases derived from tumor-infiltrating neutrophils, which are usually a major component of nonmalignant cells in tumors (27). As noted above, neutrophil-derived proteases mediate HD5 processing in the genito-urinary tract (12). On tissue sections, immunoreactive HD5 was found in specific subsets of malignant epithelial cells, the biology of which has to be further investigated. Furthermore, we demonstrated strong HD5 protein signals in sections of small-cell lung cancer tissue. Secreted HD5 appeared to accumulate in tumor stroma,

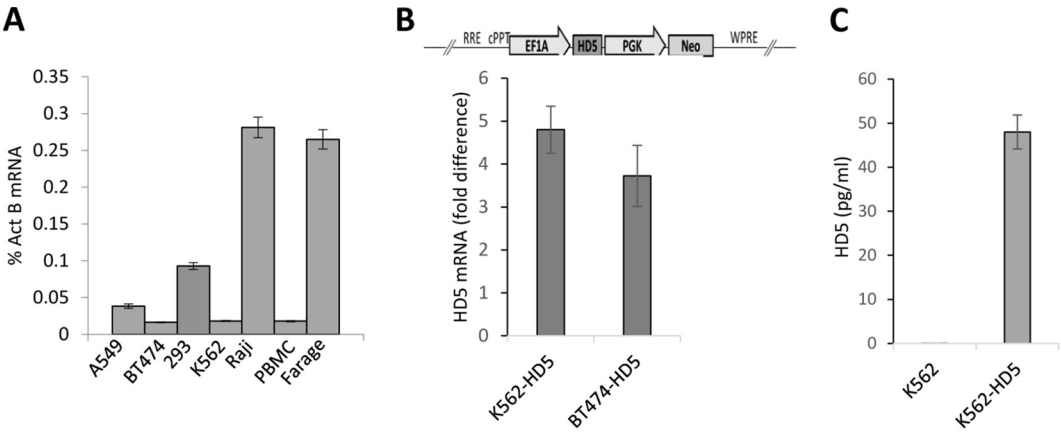

FIG 8 K562 cells with ectopic HD5 expression. (A) Screening of cell lines for endogenous HD5 expression. HD5 mRNA levels were measured in total cellular RNA by qRT-PCR and expressed as percentages of β-actin (Act B) mRNA levels. (B) HD5 mRNA expression in K562 and BT474 cells after gene transfer with an HD5-expressing lentivirus vector. The lentivirus vector contains the HD5 gene under the control of the elongation factor alpha (EF1α) promoter and the neomycin (Neo) resistance gene under the control of the phosphoglycerate kinase promoter (PGK). RRE, Rev-responsive element; cPPT, central polypurine tract; WPRE, woodchuck hepatitis virus posttranscriptional regulatory element. Cells were transduced at an MOI of 1 PFU/cell and selected with G418 for 4 weeks. HD5 and β-actin mRNA levels were measured by qRT-PCR. HD5 mRNA levels were normalized to β-actin mRNA levels and expressed as fold increase compared to the levels in parental cells ($n = 3$). (C) HD5 protein levels in supernatants of K562 and K562-HD5 cells measured by ELISA ($n = 3$).

and in some ovarian cancer patients, elevated HD5 levels were found in the serum (Fig. 10). This indicates that HD5 can come into contact with and neutralize oncolytic HAdV and potentially inhibit the intratumoral dissemination of *de novo*-produced virus. To test this hypothesis, we performed studies with HAdV3. We recently demonstrated that HAdV3 PtDd are functionally relevant for virus spread in epithelial cells (23). Immunofluorescence studies indicate that PtDd are released from infected cells before virus-triggered cytolysis and mediate restructuring of epithelial junctions. This function requires multiple Ad3 fiber knobs in a specific spatial constellation, which is present in PtDd, implying that dodecamerization is functionally important (28). Here, we report on a second function of PtDd that allows better viral dissemination, i.e., the ability of PtDd to neutralize cellular HD5 defensins. Smith et al. showed that in Ad virions HD5 molecules simultaneously bind to fiber and penton base, which upon endocytosis prevents the release of fibers and endosomal escape of virions (3). Using equilibrium binding assays with labeled HAdV5 and synthetic HD5, the same authors also concluded that several thousand HD5 molecules are bound per virus (26). Here, we show that HD5 binds to recombinant PtDd. Our SPR studies indicated a dose-dependent binding of HD5 to PtDd, with a very low dissociation rate. This is in agreement with the reported function of this peptide which is known to stabilize the viral capsid and to prevent its controlled dismantling. Direct binding of synthetic HD5 to free fiber and penton base as well as to complexes of these two proteins with higher molecular weights was also observed in a Western blot assay.

The central tool to test our hypothesis that PtDd neutralize HD5 involves the pair of wt-Ad3GFP and mut-Ad3GFP viruses. We first showed that viral spread of mut-Ad3GFP is blocked by exogenous synthetic HD5 whereas that of wt-Ad3GFP is only minimally affected. This was then further consolidated in Caco-2 cells where expression of endogenous HD5 was induced by FGF9. Finally, the ectopic expression of HD5 in K562 cells diminished the oncolytic activity of mut-Ad3GFP *in vivo* but not that of wt-Ad3GFP.

As outlined above, both viruses produce the same levels of free penton base and fiber, with the difference that mut-Ad3GFP cannot assemble pentons into dodecahedra. Our Western blot data show that HD5 binds to fiber and penton base monomers. We speculate, however, that the PtDd structure is more efficient in neutralizing HD5 than

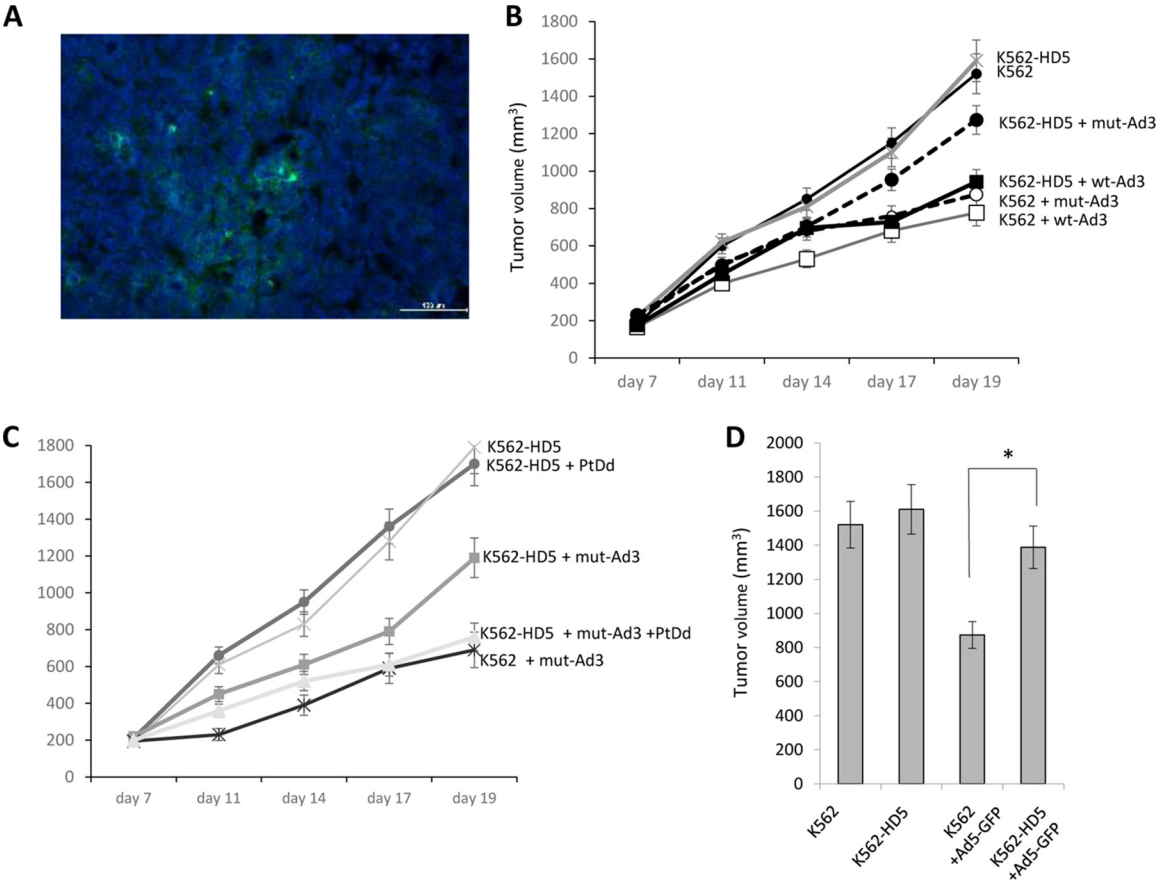

FIG 9 Effect of ectopic HD5 expression on oncolytic activity *in vivo*. (A) Mouse leukocyte infiltration of subcutaneous K562 tumors. Frozen tumor sections were stained with fluorescein isothiocyanate conjugated against the mouse pan-leukocyte marker CD45 (green). Scale bar, 100 μm. (B) *In vivo* study with wt-Ad3GFP and mut-Ad3GFP. K562 and K562-HD5 cells were injected subcutaneously to establish tumors. When tumors reached a volume of 200 mm^3, PBS, wt-Ad3GFP, or mut-Ad3GFP was injected intratumorally, and tumor volumes were measured at the indicated time points ($n = 7$). The difference between values for mut-Ad3GFP-injected K562 and K562-HD5 cells at day 19 is significant ($P < 0.05$). (C) The study described in panel A was repeated to test the effect of recombinant PtDd on the oncolytic activity of mut-Ad3GFP. Intratumoral PtDd injections (1 μg in 50 μl of PBS) were started the day after mut-Ad3GFP injection and were then repeated every 4 days. (D) *In vivo* study with wt-Ad5GFP. K562 and K562-HD5 tumors were established, and virus was injected as described for panel B. Shown are the tumor volumes at day 19 ($n = 5$). The difference between values for wt-Ad5GFP-injected K562 and K562-HD5 cells at day 19 is significant (*, $P < 0.05$).

free pentons, penton base, or fiber because mut-Ad3GFP was more sensitive to HD5 than wt-Ad3GFP. Of note, PtDd are unusual virus-like particles formed by proteins that do not interact with each other in the viral capsid where penton bases are separated by hexons. The penton/penton interface can then be considered a novel putative binding site for other interactants, such as defensins, as has been already reported for

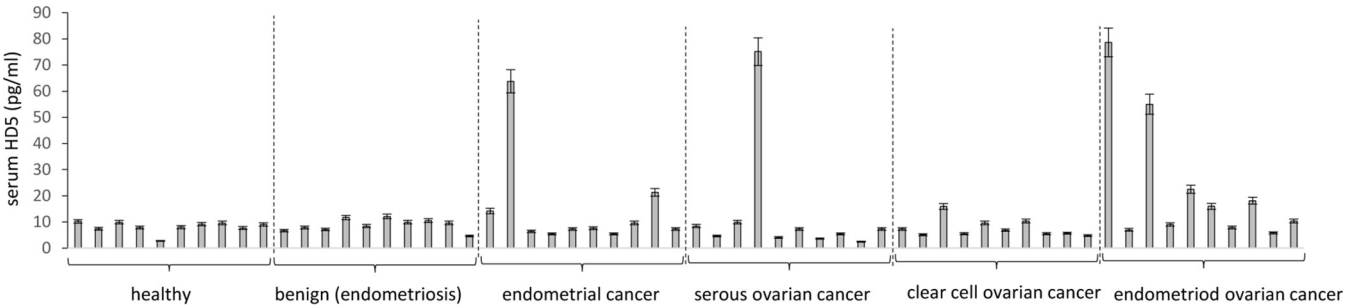

FIG 10 HD5 protein concentrations in human serum samples. Samples were diluted 1:10 in PBS and subjected to ELISA. The standard deviation is derived from technical repeats ($n = 3$).

PtDd interaction with heparan sulfate proteoglycans (HSPGs) (29). Our study suggests that HAdV serotypes that form PtDd (e.g., HAdV3, -11, and -14) could be more promising platforms for oncolytic Ad vectors.

In addition to production by colon, ovarian, endometrial, and lung cancers, it is possible that HD5 is produced by other cancers derived from epithelial cells in the airway, gastrointestinal, and genito-urinary tracts or epithelial ducts in the pancreas and liver. An indirect line of support for the association of HD5 and cancer comes from the fact that FGF9 signaling through FGFR-3 triggers HD5 expression (16). FGF9 is a target of the Wnt/β-catenin pathway. The Wnt pathway is deregulated in many types of human cancers, resulting in aberrant expression of FGF9 (30–32).

Our current findings that ovarian and lung cancers can produce HD5 and that this interferes with oncolytic activity of HAdVs are also relevant for oncolytic therapy with other viruses, including HSV, reovirus, and VSV, which are also sensitive to HD5 (13, 33). Furthermore, considering that HD5 is overexpressed in malignant endometrial cells and secreted, the peptide could theoretically serve as a cervical lavage biomarker for malignant changes in the female reproductive system.

MATERIALS AND METHODS

Reagents. Synthetic human alpha defensin HD5 peptide was from Peptide Institute, Inc. (Osaka, Japan). Recombinant FGF9 was from R&D Systems (Minneapolis, MN, USA). The HAdV3 and HAdV5 fiber knobs were produced in *Escherichia coli* with N-terminal 6-His tags using a pQE30 expression vector (Qiagen, Valencia, CA) and purified by Ni-nitrilotriacetic acid (NTA) agarose chromatography as described elsewhere (34). Recombinant Ad3 penton-dodecahedra (PtDd) were produced in insect cells and purified as described previously (35).

Adenoviruses. Propagation and purification of HAdVs were performed as described elsewhere (36). wt-Ad3GFP and wt-Ad5GFP are wild-type HAdV3- or HAdV5-based vectors containing a CMV GFP expression cassette inserted into the E3 region (23, 24). Both vectors have intact E1 genes. mut-Ad3GFP is based on wt-Ad3GFP but contains D100R and R425E mutations in the penton base gene that disable the virus's production of PtDd (23, 24). In mut-Ad3GFP, pentons (fiber plus penton base) assemble but do not form dodecameric structures.

Cell lines. Human colon cancer Caco-2 cells (ATCC HTB-37) were grown in ATCC-formulated Eagle's minimum essential medium supplemented with 20% fetal bovine serum (FBS; Gibco, Waltham, MA), 2 mM L-glutamine, antibiotics (100 IU of penicillin and 100 μg/ml streptomycin [P-S]). Human colon cancer T84 cells (ATCC CCL-284) were grown in Dulbecco's modified Eagle's medium with F12 nutrient mix (DMEM/F12) supplemented with 10% FBS, 2 mM L-glutamine, and P-S. Human HeLa, HEK 293, A549, and BT474 cell lines were grown in DMEM supplemented with 10% FBS, glutamine, and P-S. K562 and Farage cells were cultured in Iscove's modified Dulbecco's medium (IMDM) with 10% FBS, glutamine, and P-S.

Cancer biopsy specimens. Ovarian cancer biopsy specimens were obtained through the Pacific Ovarian Cancer Research Consortium (POCRC). The tissue repository provided (i) fresh or frozen tissue samples for RNA and Western blot analysis, (ii) formalin-fixed paraffin sections, and (iii) serum samples. Work with patient-derived tumor material was approved by the Fred Hutchinson Cancer Research Center Institutional Review Board (protocol 6289).

HD5 immunofluorescence. Ovarian tissue and cancer sections were embedded in optimum cutting temperature (OCT) compound (Tissue-Tek; Sakura Fineteck, Torrence, CA) and frozen on dry ice. OCT compound-embedded tissues were then stored at −80°C and equilibrated to −20°C for at least 1 h prior to sectioning. Tumor tissue was sliced (8 μm) using a Leica CM 1850 cryostat (Leica Microsystems) and then transferred onto Superfrost Plus microscope slides (Fisher Scientific, Hampton, NJ). Slides were fixed in 4% paraformaldehyde (Fisher Scientific) for 10 min at 4°C. After two rinses with phosphate-buffered saline (PBS), slides were blocked with 2% nonfat dry milk in PBS for 20 min at room temperature. Immunofluorescence analyses were performed with mouse anti-alpha defensin 5 monoclonal antibody (MAb) (MABF31; Millipore) (1:50) and goat anti-human DSG2 (AF947; R&D Systems) at 1:50. Primary antibody binding was detected with donkey anti-mouse IgG-Alexa Fluor 488 (AF488) or donkey anti-goat IgG-AF594 (1:200).

qRT-PCR for HD5 mRNA. A Quick-RNA MicroPrep kit (Zymo Research, Irvine, CA, USA) was used to extract total RNA, which was then treated with a DNA-Free kit (Ambion, Austin, TX, USA) for DNA digestion. RNA (1 μg) was reverse transcribed into cDNA using a TaqMan MicroRNA reverse transcription kit (Applied Biosystems, Foster City, CA). The qPCRs were performed using Power SYBR green master mix (Life Technologies, Carlsbad, CA). The reaction was carried out on an ABI 7300 real-time PCR system (Applied Biosystems, Foster City, CA, USA) under the following conditions: 1 cycle of 95°C for 2 min, followed by 40 cycles of 95°C for 15 s and 58°C for 60 s and a dissociation stage to generate melting curves. The sequences of the HD5-specific primers were as follows: forward primer, 5′-GGCTACAACCC AGAAGCAGT; reverse primer, 5′-CGGCCACTGATTTCACACAC. The β-actin gene (forward primer, 5′-CGT CTTCCCCTCCATCG; reverse primer, 5′-CTCGTTAATGTCACGCAC) was used as a reference gene to normalize HD5 mRNA expression. Relative expression levels were calculated using the $2^{-\Delta\Delta CT}$ (where C_T is threshold cycle) method (14).

qPCR for adenoviral DNA genomes. Genomic DNA was extracted using a DNeasy kit from Qiagen (Valencia, CA). qPCR was performed as described previously (23). The sequences of the specific primers for the adenoviral hexon detection were as follows: forward primer, 5′-GCCCCAGTGGTCATACATGCAC ATC; reverse primer, 5′-CCACGGTGGGGTTTCTAAACTT.

Inhibition of Ad transduction by synthetic HD5. wt-Ad3GFP or wt-Ad5GFP was incubated with or without synthetic HD5 at a concentration of 15 μM for 1 h at 4°C in 150 μl of DMEM serum-free medium. Confluent A549 cells were then exposed to 35 μl of the mixture (Ads with or without defensins) for 2 h at 37°C in serum-free medium. Cells were washed twice with serum-free medium and incubated with DMEM-FBS medium. After 48 h, transduction was analyzed based on GFP fluorescence by fluorescence microscopy.

Western blotting for HD5. Homogenized and sonicated tissues were incubated overnight at 4°C in 20% (wt/vol) acetic acid supplemented with protease inhibitors to extract cationic proteins. After centrifugation at 15,000 rpm in an Eppendorf centrifuge for 30 min at 4°C, supernatants were collected, and the pH was adjusted to neutral with 8 M NaOH. Ten microliters of lysate (2.5 μg of protein) was mixed with 10 μl of 2× Novex Tricine SDS sample buffer (Invitrogen, Carlsbad, CA), incubated at 85°C for 5 min, and run on a Novex 0 to 20% Tricine gel. Proteins were blotted onto a polyvinylidene difluoride (PVDF) membrane using a semidry Invitrogen iBlot system. PVDF membranes were incubated in 0.2% glutaraldehyde-PBS for 10 min, followed by 5 min of incubation in 50 mM glycine-PBS. Membranes were blocked with Tween 20–PBS–5% blocking-grade blocker (Bio-Rad, Hercules, CA) and incubated with polyclonal rabbit anti-HD5 antibodies (GTX 116079, clone N1C3; GeneTex, Irvine, CA) at a 1:1,000 dilution overnight at 4°C. Primary antibody binding was detected by anti-rabbit HRP (Cell Signaling Technology, Danvers, MA) (1:2,000). After blots were stripped with Restore Western blot striping buffer (Thermo Scientific, Waltham, MA), they were incubated with mouse anti-β-actin (Sigma, St. Louis, MO) (1:5,000). Membranes were washed five times in PBS-Tween 20 between antibody incubations, and films were developed using Amersham ECL Prime Western blotting detection reagent (GE Healthcare, Little Chalfont, United Kingdom).

HD5 ELISA. A human DEFA5 ELISA kit from Elabsciences (Wuhan, China) (E-EL-H1798) was used according to the manufacturer's directions.

Surface plasmon resonance. Binding assays were done on a BIAcore 3000 instrument. HBS-N (GE-Healthcare, Pittsburgh, PA) was used as running buffer in all experiments at a flow rate of 5 μl/min. Immobilization on a CM5 sensor chip was performed using HD5 (Peptide Institute, Inc.) at 20 μg/ml in 10 mM acetate buffer, pH 4.5, injected for 10 min on an ethyl(dimethylaminopropyl) carbodiimide/*N*-hydroxysuccinimide (EDC/NHS)-activated flow cell (570 response units [RU]). A control flow cell was activated by EDC/NHS, and both flow cells were inactivated by ethanolamine for 10 min. Different concentrations of recombinant PtDd protein were injected for a 3-min association time followed by a 2.5-min dissociation time, and the signal was automatically subtracted from the background of the ethanolamine-deactivated EDC/NHS flow cell. Kinetic and affinity constants were calculated from separated sensorgrams by the BIAeval software using a 1:1 Langmuir model.

Generation of BT474 and K562 cell lines with ectopic HD5 expression. Generation of BT474 and K562 cell lines with ectopic HD5 expression was accomplished using a VSV-G-pseudotyped lentivirus vector encoding the full-length HD5 gene under the control of the EF1α promoter (kindly provided by Xiao-Bing Zhang, Loma Linda University). For transduction of K562 cells, a 6-cm dish was coated with RetroNectin (8 μg/cm^2) for 4 h. Subsequently, the dish was blocked with 2% bovine serum albumin (BSA)-Hanks' balanced salt solution (HBSS) for 30 min at room temperature. Blocking solution was removed, and the plate was washed once with PBS. Next, the lentivirus (MOI of 10 infectious units/cell) was added to the plate for 45 min. Afterwards, K562 cells (1×10^6) were added to the plate for 4 h for infection. For the transduction of BT474 cells, 1×10^6 BT474 cells were incubated with Polybrene (4 μg/ml) and the lentivirus for 6 h. Transduced cells were incubated with 500 μg/ml of G418 for 4 weeks.

Animal studies. This study was carried out in strict accordance with the recommendations in the *Guide for the Care and Use of Laboratory Animals* endorsed by the National Institutes of Health (37). The protocol was approved by the Institutional Animal Care and Use Committee of the University of Washington, Seattle, WA (protocol 3108-01). Mice were housed in specific-pathogen-free facilities. Immunodeficient NOD.CB17-Prkdc^{scid}/J (*CB17*) mice were obtained from the Jackson Laboratory. Mice were subcutaneously injected with either K562 or K562-HD5 cells (2×10^6 cells; in Matrigel). Tumor sizes were measured every second day. After tumors reached a size of 200 mm^3, wt-Ad5GFP, wt-Ad3GFP, or mut-Ad3GFP was injected intratumorally (2×10^9 PFU/mouse).

Statistical analysis. All results are expressed as means ± standard deviations (SD). Two-way analysis of variance (ANOVA) for multiple testing was applied. Animal numbers and *P* values are indicated in the figure legends.

ACKNOWLEDGMENTS

We are grateful to Lindsay Bergan and Sarah Hawley from the POCRC specimen repository for providing the biopsy samples. We thank Matthew Horton for help in histopathology. We thank Emilie Stermann for help with the Biacore graphics.

The work was supported by NIH grant R01 HLA078836 (A.L.), a grant from the Rivkin Center for Ovarian Cancer Research (A.L.), the Pacific Ovarian Cancer Research Consortium/Specialized Program of Research Excellence in Ovarian Cancer (grant P50 CA83636 to C.D.), and a grant from the Wings of Karen Foundation (A.L.).

REFERENCES

1. Chen H, Xu Z, Peng L, Fang X, Yin X, Xu N, Cen P. 2006. Recent advances in the research and development of human defensins. Peptides 27:931–940. https://doi.org/10.1016/j.peptides.2005.08.018.
2. Wilson SS, Wiens ME, Holly MK, Smith JG. 2016. Defensins at the mucosal surface: latest insights into defensin-virus interactions. J Virol 90:5216–5218. https://doi.org/10.1128/JVI.00904-15.
3. Smith JG, Silvestry M, Lindert S, Lu W, Nemerow GR, Stewart PL. 2010. Insight into the mechanisms of adenovirus capsid disassembly from studies of defensin neutralization. PLoS Pathog 6:e1000959. https://doi.org/10.1371/journal.ppat.1000959.
4. Flatt JW, Kim R, Smith JG, Nemerow GR, Stewart PL. 2013. An intrinsically disordered region of the adenovirus capsid is implicated in neutralization by human alpha defensin 5. PLoS One 8:e61571. https://doi.org/10.1371/journal.pone.0061571.
5. Droin N, Hendra JB, Ducoroy P, Solary E. 2009. Human defensins as cancer biomarkers and antitumour molecules. J Proteomics 72:918–927. https://doi.org/10.1016/j.jprot.2009.01.002.
6. Nomura Y, Tanabe H, Moriichi K, Igawa S, Ando K, Ueno N, Kashima S, Tominaga M, Goto T, Inaba Y, Ito T, Ishida-Yamamoto A, Fujiya M, Kohgo Y. 2013. Reduction of E-cadherin by human defensin-5 in esophageal squamous cells. Biochem Biophys Res Commun 439:71–77. https://doi.org/10.1016/j.bbrc.2013.08.026.
7. Holterman DA, Diaz JI, Blackmore PF, Davis JW, Schellhammer PF, Corica A, Semmes OJ, Vlahou A. 2006. Overexpression of alpha-defensin is associated with bladder cancer invasiveness. Urol Oncol 24:97–108. https://doi.org/10.1016/j.urolonc.2005.07.010.
8. Jin G, Kawsar HI, Hirsch SA, Zeng C, Jia X, Feng Z, Ghosh SK, Zheng QY, Zhou A, McIntyre TM, Weinberg A. 2010. An antimicrobial peptide regulates tumor-associated macrophage trafficking via the chemokine receptor CCR2, a model for tumorigenesis. PLoS One 5:e10993. https://doi.org/10.1371/journal.pone.0010993.
9. Ghosh D, Porter E, Shen B, Lee SK, Wilk D, Drazba J, Yadav SP, Crabb JW, Ganz T, Bevins CL. 2002. Paneth cell trypsin is the processing enzyme for human defensin-5. Nat Immunol 3:583–590. https://doi.org/10.1038/ni797.
10. Spencer JD, Hains DS, Porter E, Bevins CL, DiRosario J, Becknell B, Wang H, Schwaderer AL. 2012. Human alpha defensin 5 expression in the human kidney and urinary tract. PLoS One 7:e31712. https://doi.org/10.1371/journal.pone.0031712.
11. Svinarich DM, Wolf NA, Gomez R, Gonik B, Romero R. 1997. Detection of human defensin 5 in reproductive tissues. Am J Obstet Gynecol 176:470–475. https://doi.org/10.1016/S0002-9378(97)70517-9.
12. Porter E, Yang H, Yavagal S, Preza GC, Murillo O, Lima H, Greene S, Mahoozi L, Klein-Patel M, Diamond G, Gulati S, Ganz T, Rice PA, Quayle AJ. 2005. Distinct defensin profiles in *Neisseria gonorrhoeae* and *Chlamydia trachomatis* urethritis reveal novel epithelial cell-neutrophil interactions. Infect Immun 73:4823–4833. https://doi.org/10.1128/IAI.73.8.4823-4833.2005.
13. Wilson SS, Wiens ME, Smith JG. 2013. Antiviral mechanisms of human defensins. J Mol Biol 425:4965–4980. https://doi.org/10.1016/j.jmb.2013.09.038.
14. Lisitsyn NA, Bukurova YA, Nikitina IG, Krasnov GS, Sykulev Y, Beresten SF. 2012. Enteric alpha defensins in norm and pathology. Ann Clin Microbiol Antimicrob 11:1. https://doi.org/10.1186/1476-0711-11-1.
15. Bousserouel S, Lamy V, Gosse F, Lobstein A, Marescaux J, Raul F. 2011. Early modulation of gene expression used as a biomarker for chemoprevention in a preclinical model of colon carcinogenesis. Pathol Int 61:80–87. https://doi.org/10.1111/j.1440-1827.2010.02621.x.
16. Brodrick B, Vidrich A, Porter E, Bradley L, Buzan JM, Cohn SM. 2011. Fibroblast growth factor receptor-3 (FGFR-3) regulates expression of Paneth cell lineage-specific genes in intestinal epithelial cells through both TCF4/beta-catenin-dependent and -independent signaling pathways. J Biol Chem 286:18515–18525. https://doi.org/10.1074/jbc.M111.229252.
17. Russell SJ, Peng KW, Bell JC. 2012. Oncolytic virotherapy. Nat Biotechnol 30:658–670. https://doi.org/10.1038/nbt.2287.
18. Kuhn I, Harden P, Bauzon M, Hermiston T. 2005. ColoAd1, a chimeric Ad11/Ad3 oncolytic virus for the treatment of colon cancer. Mol Ther 11(Suppl 1):S124. https://doi.org/10.1016/j.ymthe.2005.06.322.
19. Hemminki O, Bauerschmitz G, Hemmi S, Kanerva A, Cerullo V, Pesonen S, Hemminki A. 2010. Preclinical and clinical data with a fully serotype 3 oncolytic adenovirus Ad3-hTERT-E1A in the treatment of advanced solid tumors. Mol Ther 18(Suppl 1):S74. https://doi.org/10.1016/S1525-0016(16)37634-1.
20. Trotman LC, Achermann DP, Keller S, Straub M, Greber UF. 2003. Non-classical export of an adenovirus structural protein. Traffic 4:390–402. https://doi.org/10.1034/j.1600-0854.2003.00094.x.
21. Greber UF. 1998. Virus assembly and disassembly: the adenovirus cysteine protease as a trigger factor. Rev Med Virol 8:213–222.
22. Fender P, Boussaid A, Mezin P, Chroboczek J. 2005. Synthesis, cellular localization, and quantification of penton-dodecahedron in serotype 3 adenovirus-infected cells. Virology 340:167–173. https://doi.org/10.1016/j.virol.2005.06.030.
23. Lu ZZ, Wang H, Zhang Y, Cao H, Li Z, Fender P, Lieber A. 2013. Penton-dodecahedral particles trigger opening of intercellular junctions and facilitate viral spread during adenovirus serotype 3 infection of epithelial cells. PLoS Pathog 9:e1003718. https://doi.org/10.1371/journal.ppat.1003718.
24. Yumul R, Richter M, Lu ZZ, Saydaminova K, Wang H, Wang CH, Carter D, Lieber A. 2016. Epithelial junction opener improves oncolytic adenovirus therapy in mouse tumor models. Hum Gene Ther 27:325–337. https://doi.org/10.1089/hum.2016.022.
25. Wang H, Ducournau C, Saydaminova K, Richter M, Yumul R, Ho M, Carter D, Zubieta C, Fender P, Lieber A. 2015. Intracellular signaling and desmoglein 2 shedding triggered by human adenoviruses Ad3, Ad14, and Ad14P1. J Virol 89:10841–10859. https://doi.org/10.1128/JVI.01425-15.
26. Smith JG, Nemerow GR. 2008. Mechanism of adenovirus neutralization by Human alpha-defensins. Cell Host Microbe 3:11–19. https://doi.org/10.1016/j.chom.2007.12.001.
27. Galdiero MR, Bonavita E, Barajon I, Garlanda C, Mantovani A, Jaillon S. 2013. Tumor associated macrophages and neutrophils in cancer. Immunobiology 218:1402–1410. https://doi.org/10.1016/j.imbio.2013.06.003.
28. Wang H, Li Z, Yumul R, Lara S, Hemminki A, Fender P, Lieber A. 2011. Multimerization of adenovirus serotype 3 fiber knob domains is required for efficient binding of virus to desmoglein 2 and subsequent opening of epithelial junctions. J Virol 85:6390–6402. https://doi.org/10.1128/JVI.00514-11.
29. Vives RR, Lortat-Jacob H, Chroboczek J, Fender P. 2004. Heparan sulfate proteoglycan mediates the selective attachment and internalization of serotype 3 human adenovirus dodecahedron. Virology 321:332–340. https://doi.org/10.1016/j.virol.2004.01.015.
30. Polakis P. 2007. The many ways of Wnt in cancer. Curr Opin Genet Dev 17:45–51. https://doi.org/10.1016/j.gde.2006.12.007.
31. Hendrix ND, Wu R, Kuick R, Schwartz DR, Fearon ER, Cho KR. 2006. Fibroblast growth factor 9 has oncogenic activity and is a downstream target of Wnt signaling in ovarian endometrioid adenocarcinomas. Cancer Res 66:1354–1362. https://doi.org/10.1158/0008-5472.CAN-05-3694.
32. Todo T, Kondo T, Kirino T, Asai A, Adams EF, Nakamura S, Ikeda K, Kurokawa T. 1998. Expression and growth stimulatory effect of fibroblast growth factor 9 in human brain tumors. Neurosurgery 43:337–346. https://doi.org/10.1097/00006123-199808000-00098.
33. Lawler SE, Speranza MC, Cho CF, Chiocca EA. 21 July 2016. Oncolytic viruses in cancer treatment: a review. JAMA Oncol https://doi.org/10.1001/jamaoncol.2016.2064.
34. Wang H, Liaw YC, Stone D, Kalyuzhniy O, Amiraslanov I, Tuve S, Verlinde CL, Shayakhmetov D, Stehle T, Roffler S, Lieber A. 2007. Identification of CD46 binding sites within the adenovirus serotype 35 fiber knob. J Virol 81:12785–12792. https://doi.org/10.1128/JVI.01732-07.
35. Fender P, Ruigrok RW, Gout E, Buffet S, Chroboczek J. 1997. Adenovirus dodecahedron, a new vector for human gene transfer. Nat Biotechnol 15:52–56. https://doi.org/10.1038/nbt0197-52.
36. Tuve S, Wang H, Ware C, Liu Y, Gaggar A, Bernt K, Shayakhmetov D, Li Z, Strauss R, Stone D, Lieber A. 2006. A new group B adenovirus receptor is expressed at high levels on human stem and tumor cells. J Virol 80:12109–12120. https://doi.org/10.1128/JVI.01370-06.
37. National Research Council Committee for the Update of the Guide for the Care and Use of Laboratory Animals. 2011. Guide for the care and use of laboratory animals, 8th ed. National Academies Press, Washington, DC.